

Rational design of tandem catalysts using a core-shell structure approach

*Esteban Gioria,^{a,b} Liseth Duarte-Correa,^c Najmeh Bashiri,^a Walid Hetaba,^{c,d} Reinhard Schomäcker^e
and Arne Thomas^{*a}*

^a Technische Universität Berlin, Fakultät II, Institut für Chemie: Funktionmaterialen, Sekretariat BA2, Hardenbergstraße 40, 10623 Berlin, Germany.

^b Institute of Research on Catalysis and Petrochemistry, INCAPE, (UNL-CONICET), Santiago del Estero, 2829, 3000 Santa Fe, Argentina.

^c Fritz Haber Institute of the Max Planck Society, Department of Inorganic Chemistry, Faradayweg 4-6, 14195 Berlin, Germany.

^d Max Planck Institute for Chemical Energy Conversion, Department of Heterogeneous Reactions, Stiftstraße 34-36, 45470 Mülheim an der Ruhr, Germany

^e Technische Universität Berlin, Fakultät II, Institut für Chemie, Sekretariat TC 8, Straße des 17. Juni 124, 10623 Berlin, Germany.

Corresponding Author *e-mail: arne.thomas@tu-berlin.de

1. EXPERIMENTAL

1.1 Synthesis of silica nanospheres

To obtain monodispersed 200 nm silica nanospheres, the synthesis conditions were 3:1:0.17 M for H₂O:NH₃:TEOS (Tetraethyl orthosilicate, 99% Sigma Aldrich) using ethanol as solvent. The reaction was carried out in a 1 l round flask at 20°C under magnetic stirring at 25 rpm for 3h and the nanospheres were recovered by centrifugation (4000 rpm, 10 min). The product was washed several times with ethanol and dried overnight at 60°C, obtaining 3000 mg of nanospheres.

1.2 Synthesis of amino-functionalized silica nanospheres (SiO₂-NH₂)

The silica surface was grafted with amino groups using (3-aminopropyl)-triethoxysilane (APTES, 99% Sigma Aldrich). 1500 mg of SiO₂ nanospheres were dispersed in 285 ml of ethanol and then, 1.5 ml of APTES dissolved in 13.5 ml of ethanol was added. The reaction took place at room temperature for 24 h and the nanospheres were recovered by centrifugation (4000 rpm, 10 min). The product was washed several times with ethanol and dried overnight at 60°C.

1.3 In-situ formation of Platinum nanoparticles (SiO₂-Pt)

For the deposition of platinum nanoparticles (PtNP) onto the surface of the silica nanospheres, 1500 mg of SiO₂-NH₂ was dispersed in a mixture of 240 ml of ethanol and 22.5 ml of H₂PtCl₆ 5mM (Sigma Aldrich). After 30 min of magnetic stirring, 75 ml of NaBH₄ 0.075 mM (98%, Acros Organics) dissolved in ethanol was added. The reduction reaction took place immediately. After 15 min, the nanospheres were recovered by centrifugation (4000 rpm, 10 min) and washed several times with ethanol.

Similar conditions were employed using water as the solvent. However, large agglomerations of nanoparticles were observed (Figure S.7).

1.4 Conformation of the mesoporous silica shell (SiO₂-Pt@m-SiO₂)

For the conformation of the silica shell, 400 mg of SiO₂-Pt was suspended in 480 ml of ethanol/H₂O 50 %_{v/v} and 2 ml of NaOH 0.5 M was added. Also, 600 mg of cationic surfactant cetyltrimethylammonium bromide (CTAB, 98% Alfa Aesar) was added as a template. After mixing for 30 minutes, 600 μl TEOS dissolved in 120 ml of ethanol was added and the reaction took place at room temperature for 24 h. The nanospheres were recovered by centrifugation (4000 rpm, 10 min) and washed several times with ethanol.

To form the mesoporous structure, the organic template was removed by calcination for 2h at 350°C using a heating ramp of 5 K min⁻¹. This treatment was selected considering the thermogravimetric analysis of the CTAB under the same conditions (Figure S9).

1.5 Cobalt nanoparticles synthesis (CoNP)

Cobalt nanoparticles (CoNP) with an average size of 15.5 nm were formed by thermal decomposition of Co₂(CO)₈ following a reported protocol with slight modifications [1]. 260 mg of oleic acid (99% Sigma Aldrich) was dissolved in 30 ml of o-dichlorobenzene (99% Sigma Aldrich) and heated up to 170°C in a 250 ml round flask under nitrogen bubbling and magnetic stirring. Then, 1000 mg of Co₂(CO)₈ (90% Sigma Aldrich) dissolved in 6 ml o-dichlorobenzene was quickly injected. Instantly, the solution turns dark-reddish indicating the nanoparticle formation by thermal decomposition. The reaction took place for 20 min and after cooling down, the CoNP were precipitated using 2-propanol and recovered by centrifugation (9000 rpm, 30 min). After several washing steps to remove the organic compounds, the CoNP were easily suspended in 60 ml of hexane forming a stable colloid with a concentration of 2.8 mg Co ml⁻¹.

1.6 Formation of the final core-shell structure (SiO₂-Pt@m-SiO₂-Co)

In a final step, the pre-formed CoNP were impregnated onto the SiO₂-Pt@m-SiO₂ structure. 500 mg of SiO₂-Pt@m-SiO₂ suspended on 100 ml of hexane was mixed with a certain amount of the

CoNP suspension to obtain a final Co loading of 12 %. The suspension was mixed in a vortex for 15 min and the nanospheres were recovered by centrifugation (4000 rpm, 10 min). The solvent was evaporated at room temperature and a final calcination treatment in air (350°C – 1h – 5 K min⁻¹) was applied to remove all possible organic compounds. Following the synthesis step, the yield was 550 mg of SiO₂-Pt@m-SiO₂-Co per batch.

2. Catalytic CO₂ hydrogenation tests

The catalytic reduction of CO₂ with H₂ was settled as an accurate test reaction in order to evaluate the tandem performance of the core-shell structure. 200 mg of the sample was tested in a fixed bed reactor, (I.D. 8mm, L. 65.5 cm) using SiC as dilution support and a gas hourly space velocity GHSV = 15000 mL g⁻¹ h⁻¹. The reacting mixture gases consisted of 30 mL min⁻¹ of H₂, 10 mL min⁻¹ of CO₂, and 10 mL min⁻¹ of N₂ at 6 bar of total pressure. The catalysts were in-situ reduced for 1 h at 350 °C in a 75 % H₂ flow using a heating ramp of 10 K min⁻¹ before each catalytic test.

The catalytic activity was measured at 350 °C for at least 20 h. The reactor effluent concentrations were monitored every 30 minutes with an online Gas Chromatograph equipped with a TCD and FID detector. The CO₂ conversion and each products selectivity were calculated based on a carbon atom basis as follows, considering the composition at the inlet and outlet of the reactor [2]:

$$X_{CO_2} = \frac{CO_2^{in} - CO_2^{out}}{CO_2^{in}}$$

$$S_{CO} = \frac{CO^{out}}{CO_2^{in} - CO_2^{out}}$$

$$S_{C_nH_m} = \frac{nC_nH_m}{\sum_1^n nC_nH_m}$$

3. Characterization techniques

The morphology and size distribution of the nanospheres were analyzed by High resolution-Scanning Electron Microscopy (SEM) images using a ZEISS GeminiSEM500 NanoVP microscope. The morphology and size distribution of the nanoparticles and decorated structures were analyzed by Transmission Electron Microscopy (TEM) images using a FEI Tecnai G² 20 S-TWIN microscope operating at 200 kV.

High-Angle Annular Dark-Field-Scanning TEM (HAADF-STEM) and Energy Dispersive X-ray Spectroscopy (EDS) elemental mappings of the nanospheres at different stages of preparation were recorded in a Thermo Scientific Talos F200X microscope operated at 200 kV acceleration voltage. The microscope is equipped with a SuperX EDX detector system. Samples were prepared by dipping the lacey carbon 400-mesh copper TEM grids into the powder sample. STEM-EDS mappings show the net intensities of the correspondent elements with a prefiltering Gaussian blur of 1.5 sigma.

X-ray diffraction patterns were acquired with a Bruker D8 Advance instrument using Cu K α radiation ($\lambda = 1.54 \text{ \AA}$). X-ray photoelectron spectroscopy (XPS) was carried out in a Thermo-Fisher Scientific ESCALAB 250Xi.

Nitrogen adsorption isotherms were determined using a Quantachrome Quadrasorb SI porosimeter. The samples were degassed at 150°C for 12 h before the measurements. The surface area was calculated by using the Brunauer–Emmett–Teller (BET) equation, and the pore-sized distribution was obtained from the adsorption isotherms based on the BJH method.

Thermal gravimetric analysis (TGA) was carried out in a STA 409 apparatus (Linseis) at a temperature range of 25-800 °C, a heating rate of 5 K min⁻¹ and a flow rate of 20 mL min⁻¹ of 20% O₂/N₂.

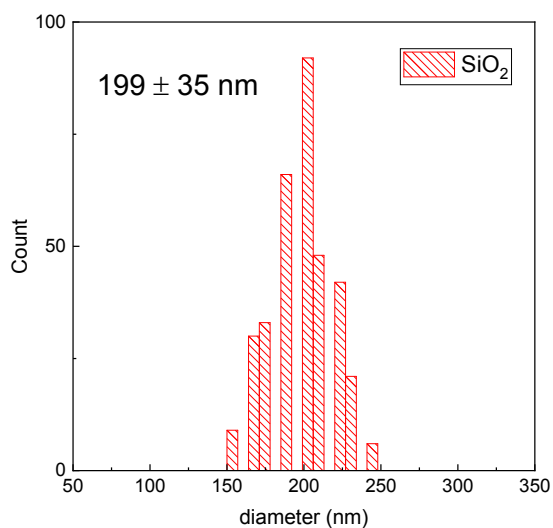
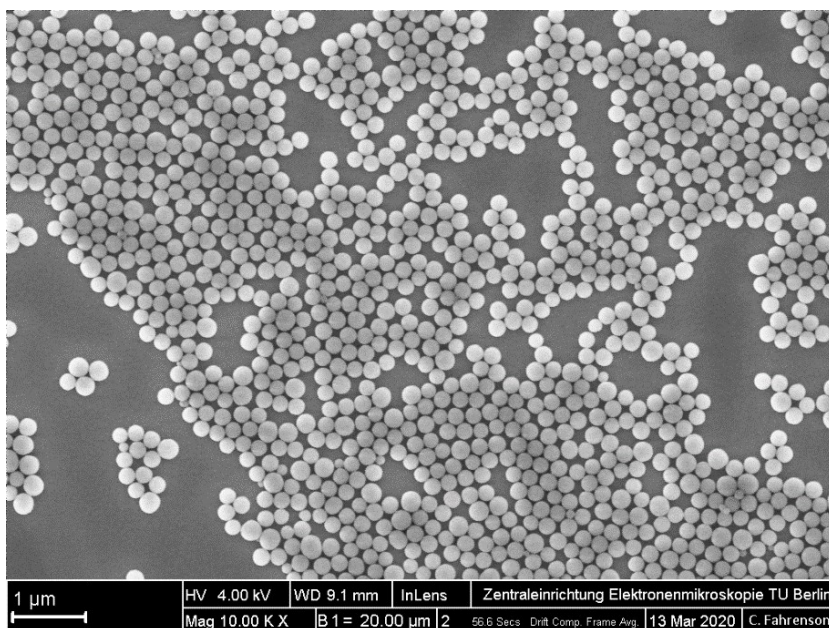


Figure S1. Scanning electron microscopy and particle size distribution of the SiO₂ nanospheres.

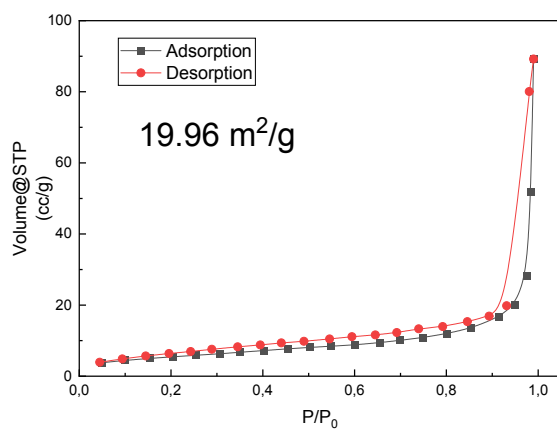


Figure S2. Nitrogen adsorption isotherms of prepared SiO₂ nanospheres.

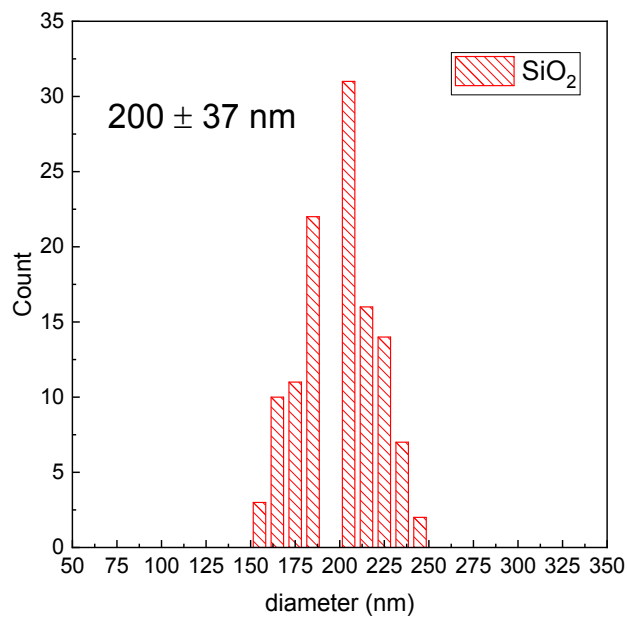
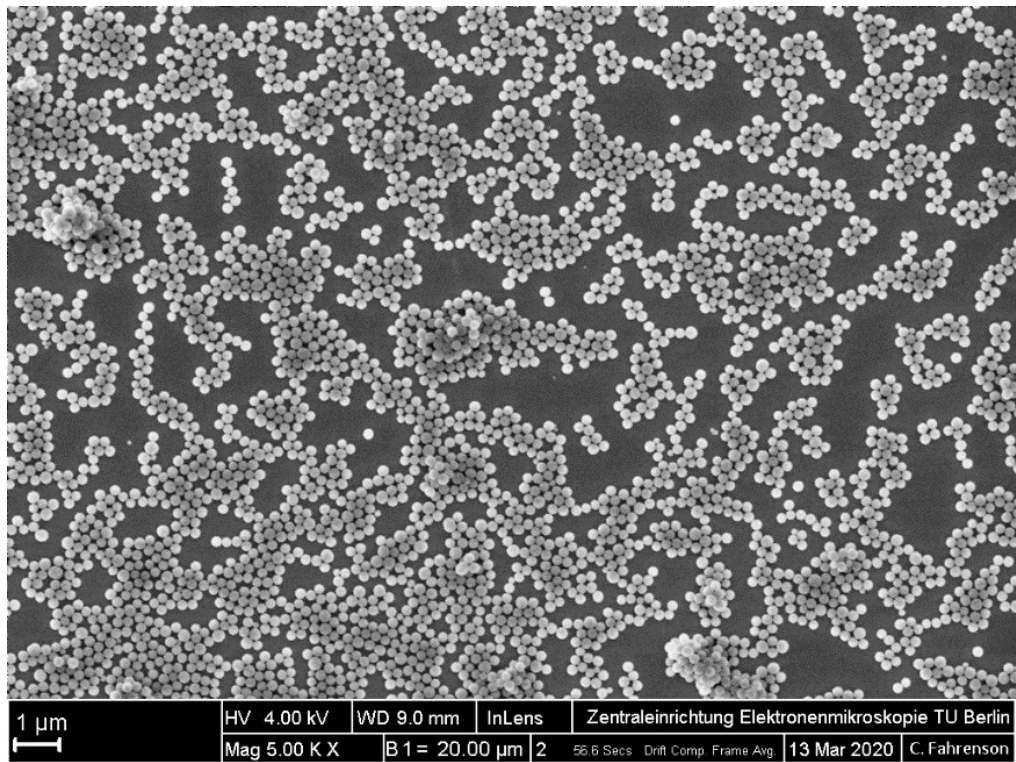


Figure S3. Scanning electron microscopy and particle size distribution of SiO₂-NH₂ nanospheres.

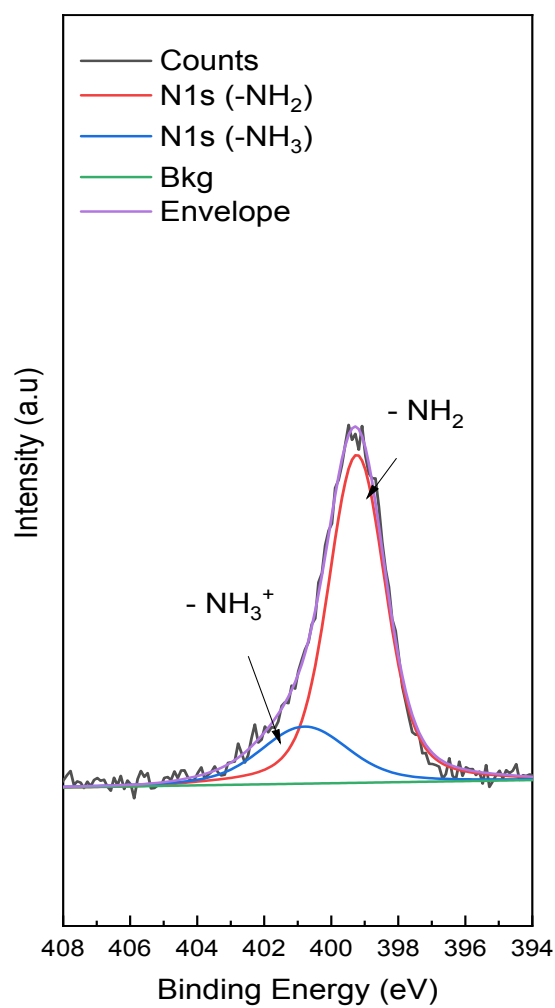


Figure S4. X-ray photoelectron spectroscopy of SiO₂-NH₂ functionalized nanospheres.

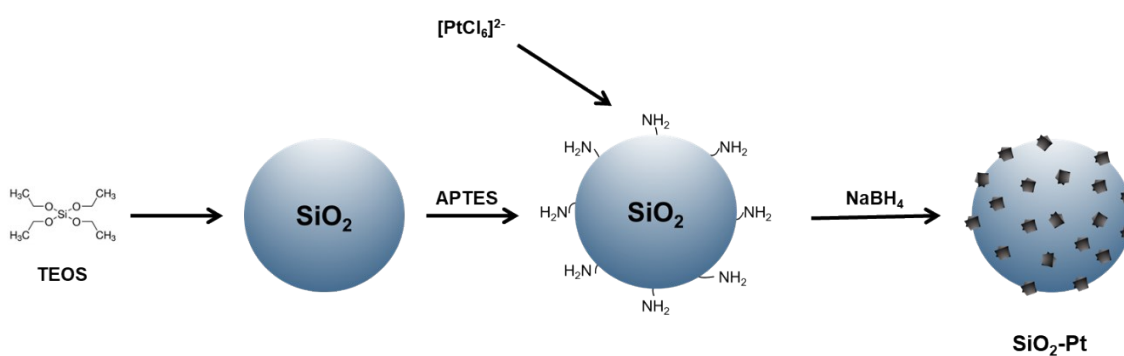


Figure S5. Schematic representation of SiO₂-Pt formation by strong electrostatic adsorption method (SEA).

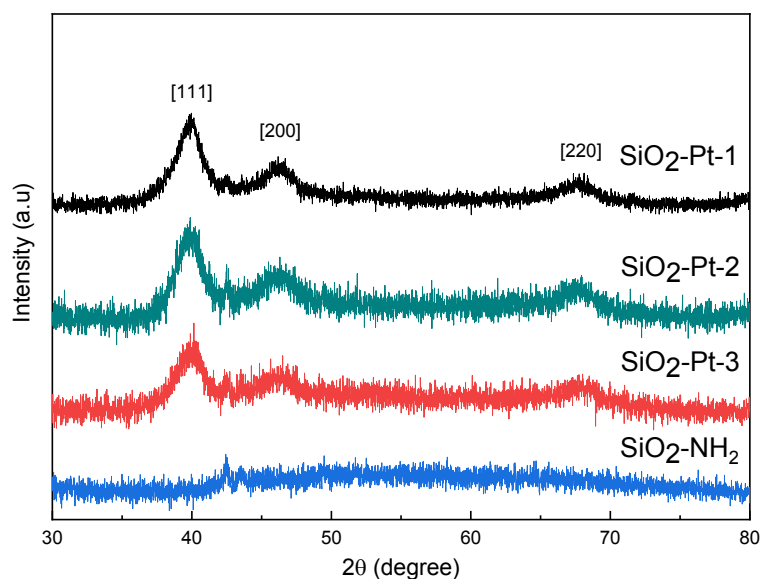


Figure S6. X-Ray diffractograms of the prepared SiO₂-Pt nanospheres obtained by different methods and solvents. SiO₂-Pt-1) using water and magnetic stirring; SiO₂-Pt-2) using ethanol and magnetic stirring; SiO₂-Pt-3) using ethanol and ultrasound (Transonic model 460/H – 35KHz).

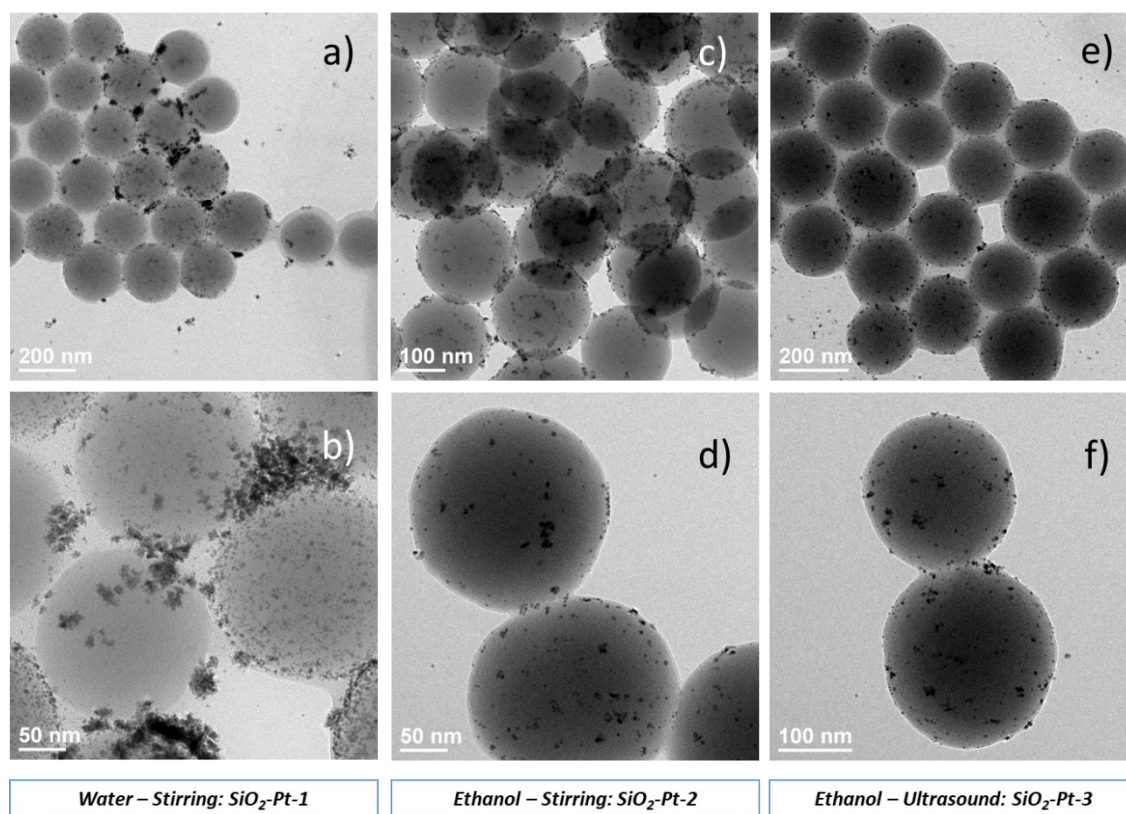


Figure S7. Transmission electron microscopy study of the SiO₂-Pt nanospheres obtained by different methods and solvents. a, b) using magnetic stirring and water; c, d) using ethanol and magnetic stirring; e, f) using ethanol and ultrasound (Transonic model 460/H – 35KHz).

When particles are synthesized in water, large agglomerates are present. Changing the solvent for ethanol notably improves the dispersion of the PtNP in the silica surface. This is attributed to the fact that the NP growth rate strongly depends on the polarity and dielectric constant of the solvent molecule [3].

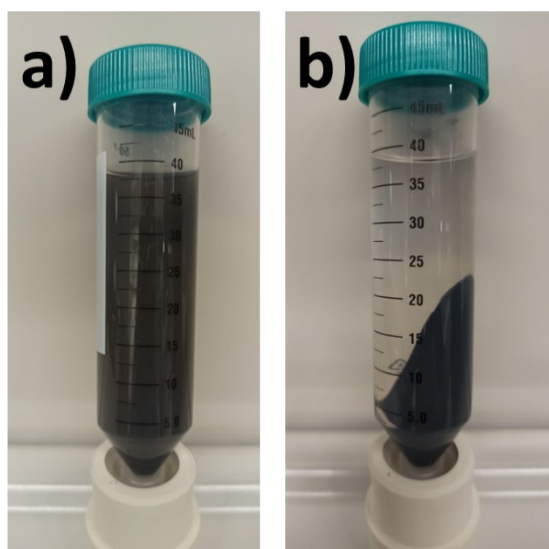


Figure S8. Facile recovery of the as-prepared SiO₂-Pt nanospheres using mild conditions (10 min – 4000 rpm). a) Before and b) after centrifugation step.

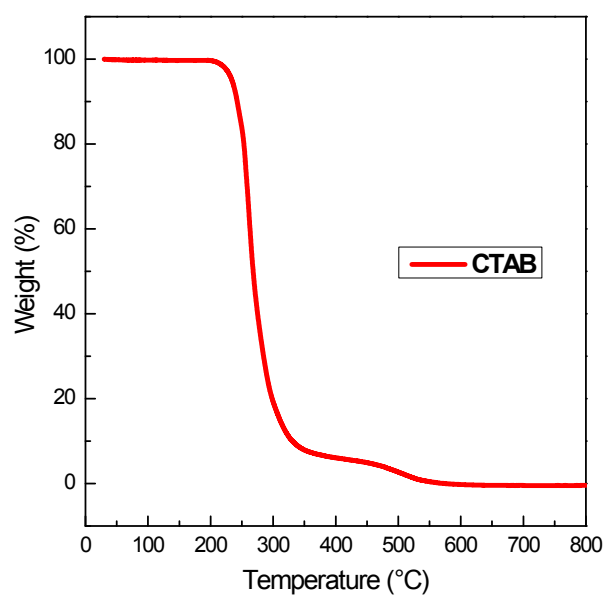


Figure S9.a. Thermogravimetric analysis (TGA) of the cetyltrimethylammonium bromide (CTAB) employed as a template. Conditions: synthetic air (20.5 % v/v O₂: N₂), gas flow of 20 ml min⁻¹, heating ramp of 5 K min⁻¹.

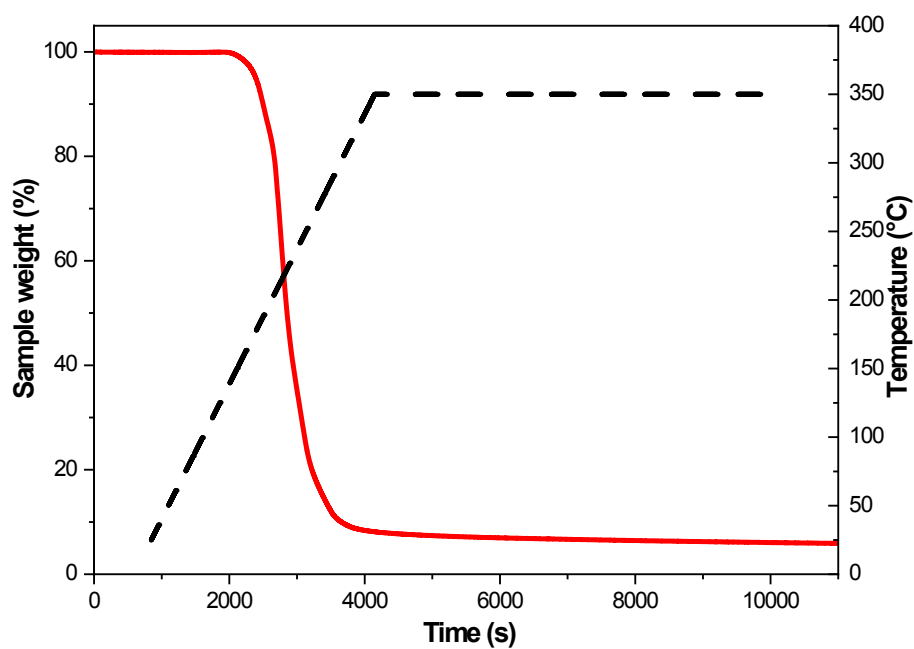


Figure S9.b. Thermogravimetric analysis (TGA) of the cetyltrimethylammonium bromide (CTAB) employed as a template. Same conditions as the calcination treatment: synthetic air (20.5 % v/v O_2 : N_2), gas flow of 20 ml min^{-1} , heating ramp of 5 K min^{-1} and d_{well} of 2h.

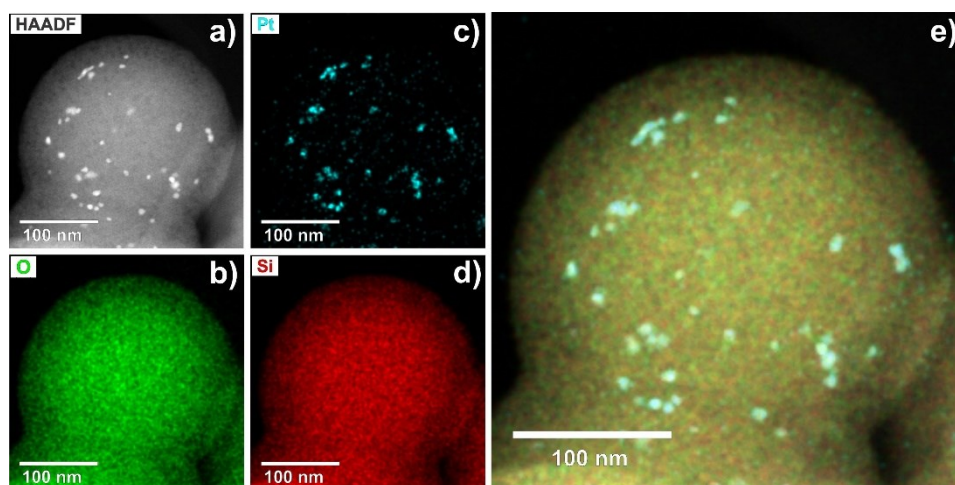


Figure S10. STEM-EDS study of the $\text{SiO}_2\text{-Pt@m-SiO}_2$ nanospheres. (a) HAADF-STEM image, elemental maps of (b) O, (c) Pt, (d) Si, and (e) mixed colored mapping.

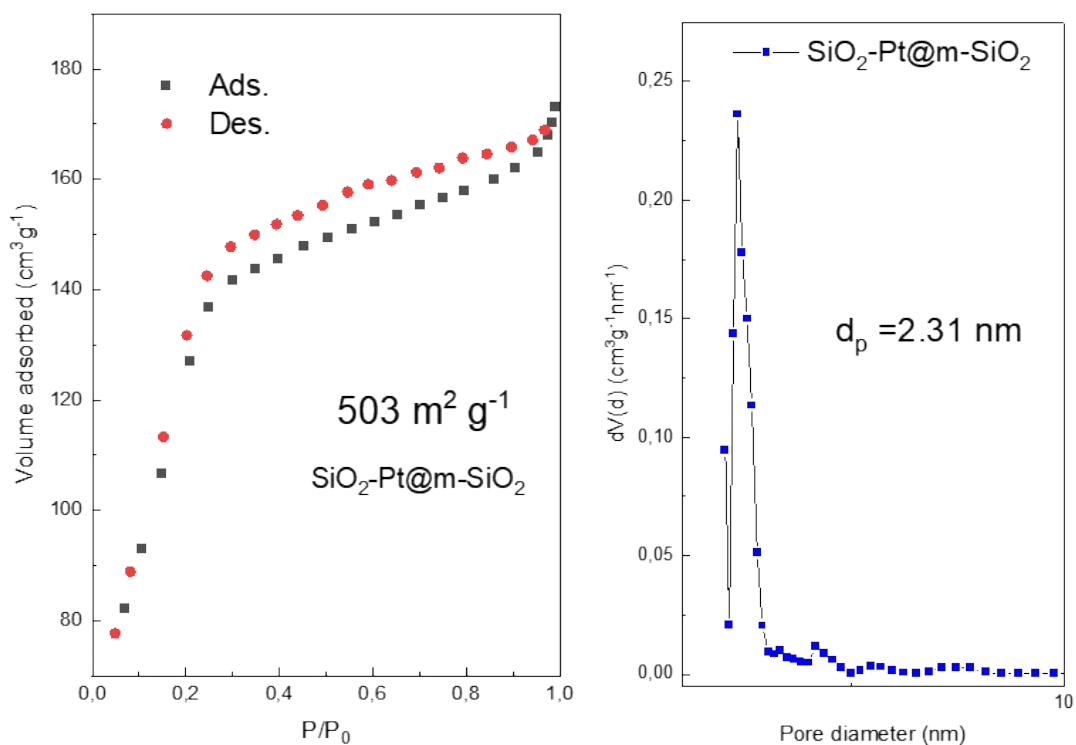


Figure S11. N_2 adsorption study of the $\text{SiO}_2\text{-Pt@m-SiO}_2$ nanospheres.

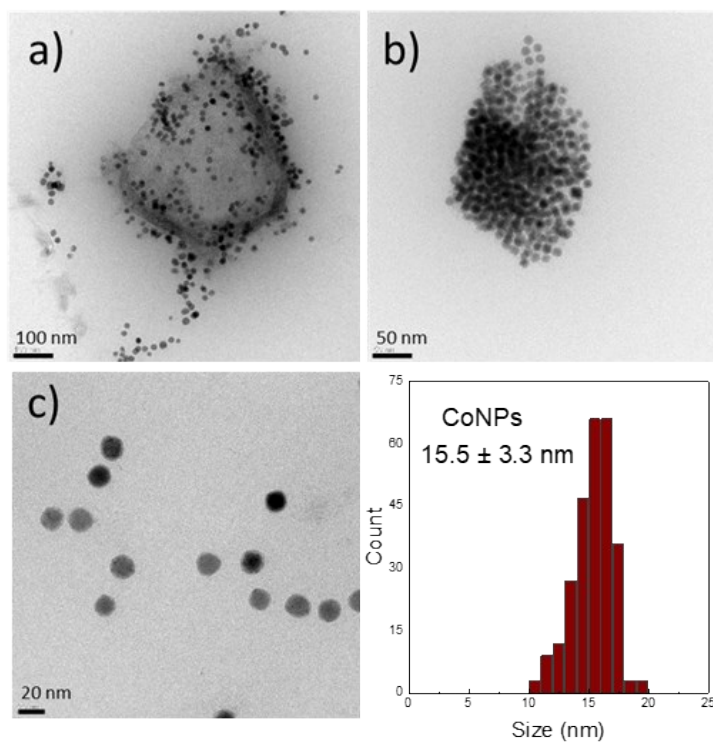


Figure S12. Transmission electron microscopy study of the cobalt nanoparticles.

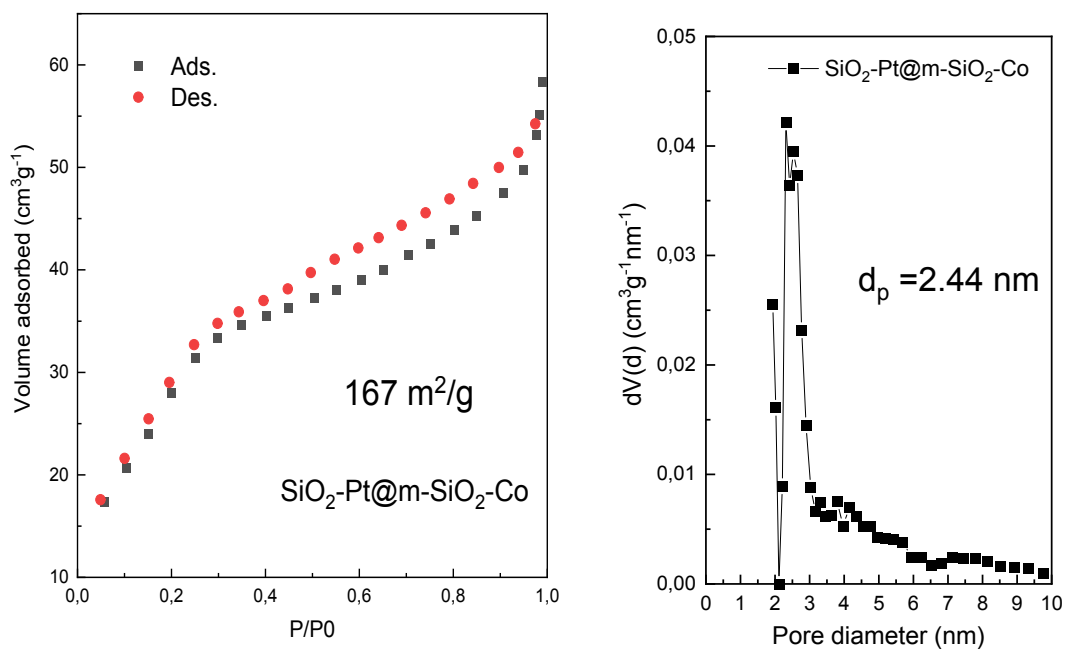


Figure S13. N_2 adsorption study of the $\text{SiO}_2\text{-Pt@m-SiO}_2\text{-Co}$ nanospheres.

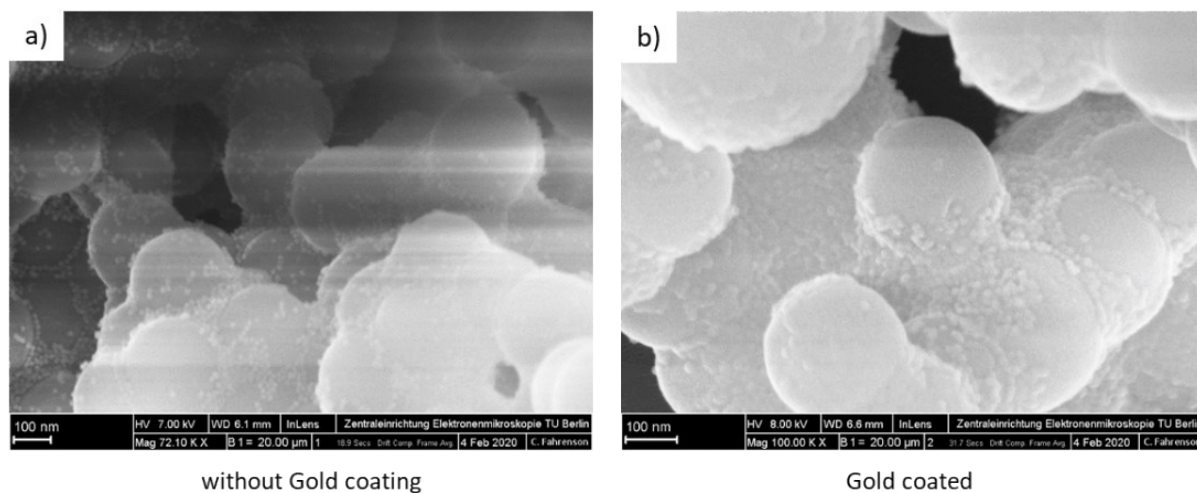


Figure S14. Scanning electron microscopy study of the $\text{SiO}_2\text{-Pt@m-SiO}_2\text{-Co}$ nanospheres; a) without gold coating and b) gold-coated nanospheres to decrease charge effects.

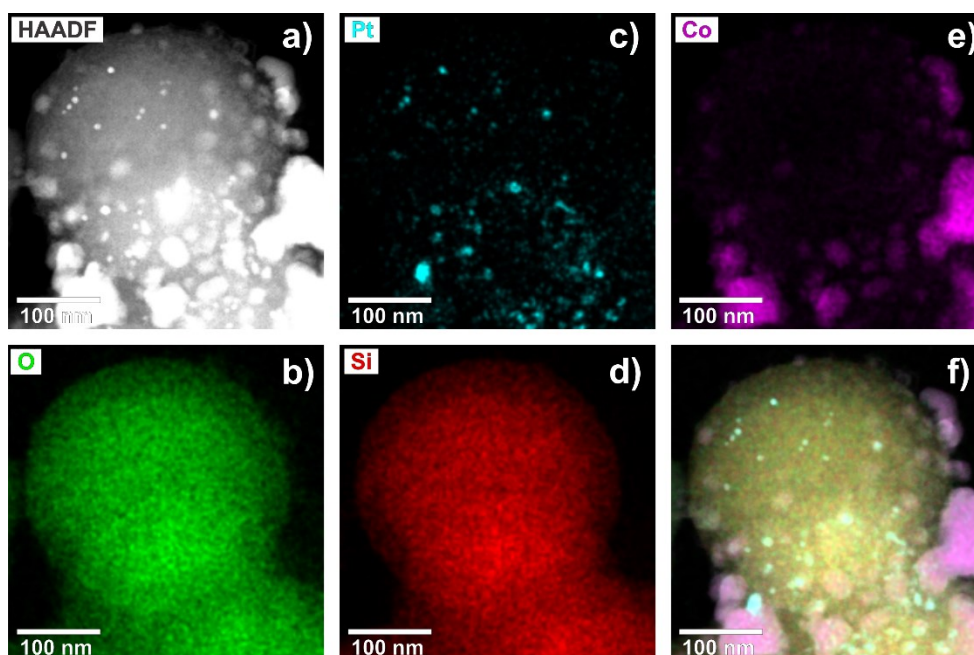


Figure S15. STEM-EDS study of the $\text{SiO}_2\text{-Pt@m-SiO}_2\text{-Co}$ nanospheres after 20h of time on stream. (a) HAADF-STEM image, elemental maps of (b) O, (c) Pt, (d) Si, (e) Co and (f) mixed colored mapping.

Figure S.15 shows no clear evidence of platinum nanoparticles agglomeration, due to the mesoporous silica shell that acts as a protective layer against sintering [4–6]. However, the high temperature and prolonged time on stream leads to migration and coalescence of the outer cobalt nanoparticles.

4. References

1. Iablokov, V.; Beaumont, S.K.; Alayoglu, S.; Pushkarev, V. V.; Specht, C.; Gao, J.; Alivisatos, A.P.; Kruse, N.; Somorjai, G.A. Size-controlled model Co nanoparticle catalysts for CO₂ hydrogenation: Synthesis, characterization, and catalytic reactions. *Nano Lett.* **2012**, *12*, 3091–3096, doi:10.1021/nl300973b.
2. Xie, C.; Chen, C.; Yu, Y.; Su, J.; Li, Y.; Somorjai, G.A.; Yang, P. Tandem Catalysis for CO₂ Hydrogenation to C₂-C₄ Hydrocarbons. *Nano Lett.* **2017**, *17*, 3798–3802, doi:10.1021/acs.nanolett.7b01139.
3. Liu, J.; Liang, C.; Zhu, X.; Lin, Y.; Zhang, H.; Wu, S. Understanding the Solvent Molecules Induced Spontaneous Growth of Uncapped Tellurium Nanoparticles. *Sci. Rep.* **2016**, *6*, 1–10, doi:10.1038/srep32631.
4. Wang, H.; Liu, M.; Ma, Y.; Gong, K.; Liu, W.; Ran, R.; Weng, D.; Wu, X.; Liu, S. Simple Strategy Generating Hydrothermally Stable Core–Shell Platinum Catalysts with Tunable Distribution of Acid Sites. *ACS Catal.* **2018**, *8*, 2796–2804, doi:10.1021/acscatal.7b04327.
5. Joo, S.H.; Park, J.Y.; Tsung, C.-K.; Yamada, Y.; Yang, P.; Somorjai, G.A. Thermally stable Pt/mesoporous silica core–shell nanocatalysts for high-temperature reactions. *Nat. Mater.* **2009**, *8*, 126–131, doi:10.1038/nmat2329.
6. Zhao, H.; Wang, D.; Gao, C.; Liu, H.; Han, L.; Yin, Y. Ultrafine platinum/iron oxide nanoconjugates confined in silica nanoshells for highly durable catalytic oxidation. *J. Mater. Chem. A* **2016**, *4*, 1366–1372, doi:10.1039/C5TA09215A.